Mathematical Modelling and Numerical Simulation with Applications, 2023, 3(2), 170–187

https://dergipark.org.tr/en/pub/mmnsa
ISSN Online: 2791-8564 / Open Access
https://doi.org/10.53391/mmnsa.1293162

RESEARCH PAPER

A Caputo-Fabrizio fractional-order cholera model and its sensitivity analysis

Idris Ahmed [1,*,‡], **Ali Akgül** [2,3,‡], **Fahd Jarad** [4,‡], **Poom Kumam** [5,‡] and **Kamsing Nonlaopon** [6,‡]

[1]Department of Mathematics, Sule Lamido University, Kafin Hausa, Jigawa State, Nigeria, [2]Department of Mathematics, Art and Science Faculty, Siirt University, 56100 Siirt, Türkiye, [3]Department of Electronics and Communication Engineering, Saveetha School of Engineering, SIMATS, Chennai, Tamilnadu, India, [4]Department of Mathematics, Cankaya University, 06790 Etimesgut, Ankara, Türkiye, [5]KMUTT Fixed Point Research Laboratory, KMUTT-Fixed Point Theory and Applications Research Group, Department of Mathematics, Faculty of Science, King Mongkut's University of Technology Thonburi (KMUTT), 126 Pracha-Uthit Road, Thrung Khru, Bangkok 10140, Thailand, [6]Department of Mathematics, Khon Kaen University, Khon Kaen 40002, Thailand

*Corresponding Author
‡idris.ahmed@slu.edu.ng (Idris Ahmed); aliakgul@siirt.edu.tr (Ali Akgül); fahd@cankaya.edu.tr (Fahd Jarad); poom.kumam@mail.kmutt.ac.th (Poom Kumam); nkamsi@kku.ac.th (Kamsing Nonlaopon)

Abstract

In recent years, the availability of advanced computational techniques has led to a growing emphasis on fractional-order derivatives. This development has enabled researchers to explore the intricate dynamics of various biological models by employing fractional-order derivatives instead of traditional integer-order derivatives. This paper proposes a Caputo-Fabrizio fractional-order cholera epidemic model. Fixed-point theorems are utilized to investigate the existence and uniqueness of solutions. A recent and effective numerical scheme is employed to demonstrate the model's complex behaviors and highlight the advantages of fractional-order derivatives. Additionally, a sensitivity analysis is conducted to identify the most influential parameters.

Keywords: Cholera; mathematical model; fixed-point theorems; sensitivity analysis; numerical simulations

AMS 2020 Classification: 26A33; 65L03; 39A60

1 Introduction

Cholera is recognized as one of the most dangerous and infectious communicable diseases, which spreads globally and poses a threat to the survival of the human population, rivaling war and

➤ **Received:** 05.05.2023 ➤ **Revised:** 28.06.2023 ➤ **Accepted:** 29.06.2023 ➤ **Published:** 30.06.2023

poverty. Infectious diseases exhibit immense diversity, and their outbreaks render millions of people vulnerable to infection, resulting in a significant economic burden on the healthcare system. Cholera is an illness transmitted through water and is characterized by a sudden onset of symptoms, including the presence of large amounts of watery diarrhea. The causative agent of the disease is known as Vibrio cholerae, a species of Gram-negative, facultative anaerobic, comma-shaped bacteria belonging to the family Vibrionaceae, with serotypes $O1$ or $O139$.
Infection with V. cholera can occur through the consumption of unhygienic water or contaminated food. People who are infected with cholera may either display symptoms or remain asymptomatic. Those who show symptoms may experience severe watery stool, vomiting, leg cramps, decreased blood pressure, kidney failure, and loss of body fluids or electrolytes (dehydration). If immediate treatment is not administered to halt these symptoms, they can potentially lead to death [1–4].
The incidence of cholera cases in Africa has been reported by the World Health Organization (WHO, 2021). The epidemic has occurred in two neighboring countries, Niger and Nigeria. In Niger Republic, the regions of Maradi and Zinder have been the most affected by cholera cases. Due to the cross-border movement of populations between these two states and Nigerian communities, many patients have been identified in Nigeria. The WHO announced that the Nigeria Centre for Disease Control (NCDC) has reported a total of 31,425 suspected cases of cholera in Nigeria since the beginning of the year 2021. Out of these cases, 311 have been confirmed, and 816 deaths have been recorded across 22 states and the Federal Capital Territory Abuja (FCT).
In modern times, mathematical modeling plays a vital role in investigating and analyzing the transmission dynamics of diseases, as well as predicting the potential impacts of intervention strategies aimed at controlling their spread. By using mathematical models, researchers can simulate various scenarios, test different interventions, and gain insights into the effectiveness of strategies for disease containment. These models help in making informed decisions and formulating policies to mitigate the dissemination of diseases, [5–11]. In recent years, there has been significant research conducted by numerous authors on the complex dynamics of the Cholera model. Theoretical analyses of such systems have resulted in a multitude of interesting findings, which have been published in various studies [12–15], along with the references cited within those publications. These authors have focused on mathematical models that describe the interactions between populations, contaminated water, and poor sanitation. By exploring these models, valuable insights into the dynamics of Cholera can be gained, contributing to a better understanding of the disease and the development of effective control strategies.
Tilahun et al. [16] developed a stochastic mathematical model to investigate the behavior of cholera disease, with a specific focus on the direct contact transmission pathway. They extensively studied the qualitative and quantitative behavior of the model. Adewole and Faniran [17] developed a human host and environment model to examine the complex dynamics of cholera infection. In their model, they considered the fraction of infectious individuals who do not adhere to treatment as part of the overall human population. Their findings suggest that while compliance with treatment is necessary, it alone is not sufficient to eradicate cholera. These studies contribute to the understanding of cholera dynamics by incorporating various factors and transmission pathways into mathematical models. The results emphasize the importance of considering both direct contact transmission and the impact of treatment adherence in devising effective strategies for cholera control.
Fractional operators, which extend the concept of differentiation and integration to non-integer orders, find extensive applications in various fields of knowledge, including physics, biology, finance, and control theory [18–25]. Their popularity has been on the rise due to their ability to model systems with complex, non-linear, and non-local behavior. One of the main advantages of

fractional operators is their capability to describe systems with memory effects, which are prevalent in physical and biological systems. Additionally, they can effectively capture the behavior of systems with long-range interactions, making them a valuable tool for modeling complex systems [26–36]. In [37], a stochastic computational model of cholera infection was proposed in the context of a direct contact transmission pathway using fractional calculus theory. The research results suggest that policymakers should consider measures such as reducing interactions, improving treatment rates, and enhancing hygiene facilities to eradicate cholera. Baleanu et al. [38] introduced a novel Caputo-Fabrizio fractional model for humans. They utilized the Picard-Lindelöf approach and fixed-point theory to explore the existence of a unique solution. Additionally, the authors demonstrated the superiority of the model over the existing model when compared to real clinical data.

2 Several fundamental concepts

In this section, we will examine some basic concepts of Caputo-Fabrizio fractional operators that are relevant to the theoretical analysis of the proposed model.
Suppose $\mathcal{H}(x_1, x_2) = \{\psi : \psi \in L^2(x_1, x_2), \text{ and } \psi' \in (x_1, x_2)\}$, where $L^2(x_1, x_2)$ is the space of square integrable functions on (x_1, x_2).

Definition 1 *[39] Suppose $\psi \in \mathcal{H}^1(x_1, x_2)$ and $\alpha \in (0, 1)$. Then*

$$ {}^{CF}D^{\alpha}_{\kappa}\psi(\kappa) = \frac{\mathcal{M}(\alpha)}{1-\alpha}\int_{x_1}^{\kappa}\psi'(y)\exp\left[-\alpha\frac{\kappa-y}{1-\alpha}\right]dy, \tag{1}$$

is defined as the Caputo-Fabrizio fractional derivative, where $\mathcal{M}(\alpha)$ is a normalization function with $\mathcal{M}(0) = M(1) = 1$. In addition, if $\psi \notin \mathcal{H}^1(x_1, x_2)$ then (1) gives

$$ {}^{CF}D^{\alpha}_{\kappa}\psi(\kappa) = \frac{\alpha\mathcal{M}(\alpha)}{1-\alpha}\int_{x_1}^{\kappa}(\psi(\kappa)-\psi(y))\exp\left[-\alpha\frac{\kappa-y}{1-\alpha}\right]dy. \tag{2}$$

Remark 1 *Setting $p = \frac{1-\alpha}{\alpha} \in (0, \infty)$, then $\alpha = \frac{1}{1+p} \in (0, 1)$. In view of (2), we have*

$$ {}^{CF}D^{\alpha}_{\kappa}\psi(\kappa) = \frac{\mathcal{N}(p)}{p}\int_{x_1}^{\kappa}\psi'(y)\exp\left[\frac{\kappa-y}{p}\right]dy, \tag{3}$$

where $\mathcal{N}(p)$ is a normalization term similar to $\mathcal{M}(\alpha)$ and $\mathcal{N}(0) = \mathcal{N}(\infty) = 1$.

Remark 2 *The relation:*

$$ \lim_{p\to 0}\frac{1}{p}\exp\left[\frac{\kappa-y}{p}\right] = \delta(y-\kappa), \tag{4}$$

is true, where $\delta(y-\kappa)$ is the Dirac delta function.

Losada and Nioto [39] modified Definition 1, as

$$ {}^{CF}D^{\alpha}_{\kappa}\psi(\kappa) = \frac{(2-\alpha)}{2(1-\alpha)}\int_{x_1}^{\kappa}\psi'(y)\exp\left[-\alpha\frac{\kappa-y}{1-\alpha}\right]dy, \tag{5}$$

while its corresponding fractional integral is as follows:

Definition 2 *Suppose* $0 < \alpha < 1$, *where* α *is order of the integral. Then*

$$ {}^{CF}I_{\kappa}^{\alpha}\psi(\kappa) = \frac{2(1-\alpha)}{(2-\alpha)\mathcal{M}(\alpha)}\psi(\kappa) + \frac{2\alpha}{(2-\alpha)\mathcal{M}(\alpha)}\int_0^{\kappa}\psi(y)dy, \quad \kappa \geq x_1, \tag{6} $$

is referred as Caputo-Fabrizio fractional integral of a function ψ.

Remark 3 *From* (6), *the Caputo-Fabrizio fractional integral of a function* ψ *of order* $0 < \alpha < 1$ *is a mean between the function* ψ *and its integral of order one, i.e.,*

$$ \frac{2(1-\alpha)}{(2-\alpha)\mathcal{M}(\alpha)} + \frac{2\alpha}{(2-\alpha)\mathcal{M}(\alpha)} = 1, $$

thus, $\mathcal{M}(\alpha) = \frac{2}{2-\alpha}$, $0 < \alpha < 1$.

If $\mathcal{M}(\alpha) = \frac{2}{2-\alpha}$, then the new Caputo derivative and its corresponding integral as follows [39]:

Definition 3 *Let* $0 < \alpha < 1$, *then*

$$ {}^{CF}D_{\kappa}^{\alpha}\psi(\kappa) = \frac{1}{1-\alpha}\int_{x_1}^{\kappa}\psi'(y)\exp\left[-\alpha\frac{\kappa-y}{1-\alpha}\right]dx, \quad \kappa \geq x_1, \tag{7} $$

and its fractional integral as:

$$ {}^{CF}I_{\kappa}^{\alpha}\psi(\kappa) = (1-\alpha)\psi(\kappa) + \alpha\int_{x_1}^{\kappa}\psi(y)dy, \quad \kappa \geq x_1, \tag{8} $$

respectively, are referred as Caputo-Fabrizio fractional derivative and fractional integral of order α *of a function* ψ.

3 Description of the model

We study the Cholera model as proposed in [40]. The classical Cholera model is formulated by the following system:

$$ \begin{aligned} \frac{dS(\kappa)}{d\kappa} &= \Omega - (\lambda I - \mu)S + \eta V + \gamma R, \\ \frac{dI(\kappa)}{d\kappa} &= \lambda SI - (\mu + \omega + \sigma + \beta)I, \\ \frac{dR(\kappa)}{d\kappa} &= \beta I - (\mu + \gamma)R, \\ \frac{dV(\kappa)}{d\kappa} &= \sigma I - \eta V. \end{aligned} \tag{9} $$

Thus, the Caputo-Fabrizio fractional-order model is given by:

$$ \begin{aligned} {}^{CF}D^{\alpha}S &= \Omega - \lambda SI - \mu S + \eta V + \gamma R, \\ {}^{CF}D^{\alpha}I &= \lambda SI - \mu I - \omega I - \sigma I - \beta I, \\ {}^{CF}D^{\alpha}R &= \beta I - \mu R - \gamma R, \\ {}^{CF}D^{\alpha}V &= \sigma I - \eta V, \end{aligned} \tag{10} $$

Table 1. States variables

Compartment	Description
S	Susceptible population
I	Symptomatic infected population with Cholera
R	Recovered population
V	Environment

Table 2. Meaning of each parameters.

Parameters	Biological Meanings
Ω	Population recruitment rate
λ	Contact rate
β	Recovery rate
ω	Death rate due infection
γ	Loose of immunity
μ	Natural death rate
σ	Rate of infection among compartment I and V
η	Rate of infection among compartment V and S

subject to

$$S(0) = S_0 \geq 0,\ I(0) = I_0 \geq 0,\ R(0) = R_0 \geq 0,\ \text{and}\ V(0) = V_0 \geq 0. \tag{11}$$

Tables 1 and 2 display the biological meaning of each state variable and parameters used in the model, respectively.

4 Qualitative analysis of the model

This section uses fixed point theorems to explore the existence and uniqueness of solutions to the proposed model (10).

Existence and uniqueness result

By utilizing the fixed point theorems, this subsection aims to demonstrate the existence and uniqueness of model (10). To facilitate this analysis, model (10) can be expressed as follows:

$$\begin{aligned} {}^{CF}D^{\alpha}S &= \mathcal{K}_1(\kappa, S), \\ {}^{CF}D^{\alpha}I &= \mathcal{K}_2(\kappa, I), \\ {}^{CF}D^{\alpha}R &= \mathcal{K}_3(\kappa, R), \\ {}^{CF}D^{\alpha}V &= \mathcal{K}_4(\kappa, V), \end{aligned} \tag{12}$$

where

$$\begin{aligned} \mathcal{K}_1(\kappa, S) &= \Omega - \lambda SI - \mu S + \eta V + \gamma R, \\ \mathcal{K}_2(\kappa, I) &= \lambda SI - \mu I - \omega I - \sigma I - \beta I, \\ \mathcal{K}_3(\kappa, R) &= \beta I - \mu R - \gamma R, \\ \mathcal{K}_4(\kappa, V) &= \sigma I - \eta V. \end{aligned} \tag{13}$$

Applying fractional integral operator given in (6), system (12) reduces to the Volterra integral type of order $(0 < \alpha < 1)$ given by

$$\begin{aligned}
S(\kappa) &= S(0) + 2\frac{(1-\alpha)}{(2-\alpha)\mathcal{M}(\alpha)}\mathcal{K}_1(\kappa, S) + 2\frac{\alpha}{(2-\alpha)\mathcal{M}(\alpha)}\int_0^\kappa \mathcal{K}_1(y, S)dy,\\
I(\kappa) &= I(0) + 2\frac{(1-\alpha)}{(2-\alpha)\mathcal{M}(\alpha)}\mathcal{K}_2(\kappa, I) + 2\frac{\alpha}{(2-\alpha)\mathcal{M}(\alpha)}\int_0^\kappa \mathcal{K}_2(y, I)dy,\\
R(\kappa) &= R(0) + 2\frac{(1-\alpha)}{(2-\alpha)\mathcal{M}(\alpha)}\mathcal{K}_3(\kappa, R) + 2\frac{\alpha}{(2-\alpha)\mathcal{M}(\alpha)}\int_0^\kappa \mathcal{K}_3(y, R)dy,\\
V(\kappa) &= V(0) + 2\frac{(1-\alpha)}{(2-\alpha)\mathcal{M}(\alpha)}\mathcal{K}_4(\kappa, V) + 2\frac{\alpha}{(2-\alpha)\mathcal{M}(\alpha)}\int_0^\kappa \mathcal{K}_4(y, V)dy.
\end{aligned} \tag{14}$$

Next, under some assumptions, we demonstrate that the kernels $\mathcal{K}_1$, $\mathcal{K}_2$, $\mathcal{K}_3$ and $\mathcal{K}_4$ obey the Lipschitz and contraction conditions. To do so, we state and prove the following lemma.

Lemma 1 *The autonomous system* (13) *is Lipschitz continuous.*

Proof For S and S^*, we have from (13), gives

$$\begin{aligned}
\|\mathcal{K}_1(\kappa, S) - \mathcal{K}_1(\kappa, S^*)\| &= \|\lambda I(t)(S(\kappa) - S^*(\kappa)) - \mu(S(\kappa) - S^*(\kappa))\|\\
&\leq \|\lambda I(\kappa)\|\|S(\kappa) - S^*(\kappa)\| + \mu\|S(\kappa) - S^*(\kappa)\|\\
&\leq (\epsilon\lambda + \mu)\|S(\kappa) - S^*(\kappa)\|\\
&\leq l_1\|S(\kappa) - S^*(\kappa)\|,
\end{aligned}$$

where $0 < l_1 = (\epsilon\lambda + \mu)$ *and* $\|I(\kappa)\| \leq \epsilon$ is bounded.
For I and I^*, we have

$$\begin{aligned}
\|\mathcal{K}_2(\kappa, I) - \mathcal{K}_2(I^*)\| &= \|(\lambda S - \mu - \omega - \sigma - \beta)(I(\kappa) - I^*(\kappa))\|\\
&\leq (\|\lambda S\| + (\mu + \omega + \sigma + \beta))\|(I(\kappa) - I^*(\kappa))\|\\
&\leq l_2\|(I(\kappa) - I^*(\kappa))\|,
\end{aligned}$$

where $0 < l_2 = (\lambda\epsilon_1 + (\mu + \omega + \sigma + \beta))$ *and* $\|S(\kappa)\| \leq \epsilon_1$ is bounded.
From R and R^*, we have

$$\begin{aligned}
|\mathcal{K}_3(R) - \mathcal{K}_3(R^*)| &= \| - (\mu + \gamma)(R(\kappa) - R^*(\kappa))\|\\
&\leq (\mu + \gamma)|(R(\kappa) - R^*(\kappa))\|\\
&\leq l_3\|R(\kappa) - R^*(\kappa)\|,
\end{aligned}$$

where $0 < l_3 = (\mu + \gamma)$.
From V and V^*, we have

$$\begin{aligned}
|\mathcal{K}_4(V) - \mathcal{K}_4(V^*)| &= \| - \eta(V(\kappa) - V^*(\kappa))\|\\
&\leq l_4\|(V(\kappa) - V^*(\kappa)\|,
\end{aligned}$$

where $0 < l_4 = \eta$. Hence it's Lipschitz continuous and the proof of the lemma is complete. ■
Now, system (14) can be written in recursive form by the difference between the successive terms

as given below:

$$\begin{aligned}
\chi_{1n} &= S_n(\kappa) - S_{n-1}(\kappa) = \frac{2(1-\alpha)}{(2-\alpha)\mathcal{M}(\alpha)}(\mathcal{K}_1(\kappa, S_{n-1}) - \mathcal{K}_1(\kappa, S_{n-2})) \\
&\quad + 2\frac{\alpha}{(2-\alpha)\mathcal{M}(\alpha)}\int_0^\kappa (\mathcal{K}_1(\kappa, S_{n-1}) - \mathcal{K}_1(\kappa, S_{n-2}))dy, \\
\chi_{2n} &= I_n(\kappa) - I_{n-1}(\kappa) = \frac{2(1-\alpha)}{(2-\alpha)\mathcal{M}(\alpha)}(\mathcal{K}_2(\kappa, I_{n-1}) - \mathcal{K}_2(\kappa, I_{n-2})) \\
&\quad + 2\frac{\alpha}{(2-\alpha)\mathcal{M}(\alpha)}\int_0^\kappa (\mathcal{K}_2(\kappa, I_{n-1}) - \mathcal{K}_2(\kappa, I_{n-2}))dy, \\
\chi_{3n} &= R_n(\kappa) - R_{n-1}(\kappa) = \frac{2(1-\alpha)}{(2-\alpha)\mathcal{M}(\alpha)}(\mathcal{K}_3(\kappa, R_{n-1}) - \mathcal{K}_3(\kappa, R_{n-2})) \\
&\quad + 2\frac{\alpha}{(2-\alpha)\mathcal{M}(\alpha)}\int_0^\kappa (\mathcal{K}_3(\kappa, R_{n-1}) - \mathcal{K}_3(\kappa, R_{n-2}))dy, \\
\chi_{4n} &= V_n(\kappa) - V_{n-1}(\kappa) = \frac{2(1-\alpha)}{(2-\alpha)\mathcal{M}(\alpha)}(\mathcal{K}_4(\kappa, V_{n-1}) - \mathcal{K}_4(\kappa, V_{n-2})) \\
&\quad + 2\frac{\alpha}{(2-\alpha)\mathcal{M}(\alpha)}\int_0^\kappa (\mathcal{K}_4(\kappa, V_{n-1}) - \mathcal{K}_4(\kappa, V_{n-2}))dy,
\end{aligned} \tag{15}$$

subject to initial conditions $S_0(\kappa) = S(0),\ I_0(\kappa) = I(0),\ R_0(\kappa) = R(0),\ V_0(\kappa) = V(0)$. From the first equation in (15), taking norm and applying triangular inequality yields:

$$\begin{aligned}
\|S_n(\kappa) - S_{n-1}(\kappa)\| &= \frac{2(1-\alpha)}{(2-\alpha)\mathcal{M}(\alpha)}\|(\mathcal{K}_1(\kappa, S_{n-1}) - \mathcal{K}_1(\kappa, S_{n-2}))\| \\
&\quad + 2\frac{\alpha}{(2-\alpha)\mathcal{M}(\alpha)}\int_0^t \|(\mathcal{K}_1(\kappa, S_{n-1}) - \mathcal{K}_1(\kappa, S_{n-2}))\|dy.
\end{aligned} \tag{16}$$

In view of Lemma 1, we get

$$\begin{aligned}
\|S_n(\kappa) - S_{n-1}(\kappa)\| &= \frac{2(1-\alpha)}{(2-\alpha)\mathcal{M}(\alpha)}l_1\|S_{n-1} - S_{n-2}\| \\
&\quad + \frac{2\alpha}{(2-\alpha)\mathcal{M}(\alpha)}l_1\int_0^\kappa \|S_{n-1} - S_{n-2}\|dy.
\end{aligned} \tag{17}$$

Therefore, we obtain

$$\|\chi_{1n}(\kappa)\| \leq \frac{2(1-\alpha)}{(2-\alpha)\mathcal{M}(\alpha)}l_1\|\chi_{1(n-1)}(\kappa)\| + \frac{2\alpha}{(2-\alpha)\mathcal{M}(\alpha)}l_1\int_0^\kappa \|\chi_{1(n-1)}(y)\|dy. \tag{18}$$

Thus, the rest of the equations in system (15) can be obtained in the same approach as:

$$\begin{aligned}
\|\chi_{2n}(\kappa)\| &\leq \frac{2(1-\alpha)}{(2-\alpha)\mathcal{M}(\alpha)}l_1\|\chi_{2(n-1)}(\kappa)\| + \frac{2\alpha}{(2-\alpha)\mathcal{M}(\alpha)}l_1\int_0^\kappa \|\chi_{2(n-1)}(y)\|dy, \\
\|\chi_{3n}(\kappa)\| &\leq \frac{2(1-\alpha)}{(2-\alpha)\mathcal{M}(\alpha)}l_1\|\chi_{3(n-1)}(\kappa)\| + \frac{2\alpha}{(2-\alpha)\mathcal{M}(\alpha)}l_1\int_0^\kappa \|\chi_{3(n-1)}(y)\|dy, \\
\|\chi_{4n}(\kappa)\| &\leq \frac{2(1-\alpha)}{(2-\alpha)\mathcal{M}(\alpha)}l_1\|\chi_{4(n-1)}(\kappa)\| + \frac{2\alpha}{(2-\alpha)\mathcal{M}(\alpha)}l_1\int_0^\kappa \|\chi_{4(n-1)}(y)\|dy.
\end{aligned} \tag{19}$$

Hence, we have

$$\begin{cases} S_n(\kappa) = \sum_{k=1}^{n} \chi_{1k}(\kappa), \\ I_n(\kappa) = \sum_{k=1}^{n} \chi_{2k}(\kappa), \\ R_n(\kappa) = \sum_{k=1}^{n} \chi_{3k}(\kappa), \\ V_n(\kappa) = \sum_{k=1}^{n} \chi_{4k}(\kappa). \end{cases} \tag{20}$$

The following theorem guarantees the existence of the solution.

Theorem 1 *Consider the model given by (10), then there exist a solution if one can find κ_1 for which*

$$\frac{2(1-\alpha)}{(2-\alpha)\mathcal{M}(\alpha)} l_k + \frac{2\alpha\kappa_1}{(2-\alpha)\mathcal{M}(\alpha)} l_k < 1, \quad k = 1, 2, \ldots, 4,$$

holds.

Proof From Lemma 1 and Eqs. (18) and (19), applying the recursive technique we obtained below:

$$\begin{aligned} \|\chi_{1n}(\kappa)\| &\leq \|S_n(0)\| \left[\frac{2(1-\alpha)}{(2-\alpha)\mathcal{M}(\alpha)} l_1 + \frac{2\alpha\kappa_1}{(2-\alpha)\mathcal{M}(\alpha)} l_1 \right]^n, \\ \|\chi_{2n}(\kappa)\| &\leq \|I_n(0)\| \left[\frac{2(1-\alpha)}{(2-\alpha)\mathcal{M}(\alpha)} l_2 + \frac{2\alpha\kappa_1}{(2-\alpha)\mathcal{M}(\alpha)} l_2 \right]^n, \\ \|\chi_{3n}(\kappa)\| &\leq \|R_n(0)\| \left[\frac{2(1-\alpha)}{(2-\alpha)\mathcal{M}(\alpha)} l_3 + \frac{2\alpha\kappa_1}{(2-\alpha)\mathcal{M}(\alpha)} l_3 \right]^n, \\ \|\chi_{4n}(\kappa)\| &\leq \|V_n(0)\| \left[\frac{2(1-\alpha)}{(2-\alpha)\mathcal{M}(\alpha)} l_4 + \frac{2\alpha\kappa_1}{(2-\alpha)\mathcal{M}(\alpha)} l_4 \right]^n. \end{aligned} \tag{21}$$

This shows that the system solution exists and is continuous. Next, we show that (21) constructs the solution for the model (10), we proceed as follows:

$$\begin{aligned} S(t) - S(0) &= S_n(\kappa) - \mathcal{B}_{1n}(\kappa), \\ I(t) - I(0) &= I_n(\kappa) - \mathcal{B}_{2n}(\kappa), \\ R(t) - R(0) &= R_n(\kappa) - \mathcal{B}_{3n}(\kappa), \\ V(t) - V(0) &= V_n(\kappa) - \mathcal{B}_{4n}(\kappa). \end{aligned} \tag{22}$$

Thus, we obtain

$$\begin{aligned} \|\mathcal{B}_{1n}(\kappa)\| &= \left\| \frac{2(1-\alpha)}{(2-\alpha)\mathcal{M}(\alpha)} (\mathcal{K}_1(\kappa, S) - \mathcal{K}_1(\kappa, S_{n-1})) \right. \\ &\quad \left. + \frac{2\alpha}{(2-\alpha)\mathcal{M}(\alpha)} \int_0^\kappa (\mathcal{K}_1(\kappa, S) - \mathcal{K}_1(\kappa, S_{n-1}))dy \right\| \\ &\leq \frac{2(1-\alpha)}{(2-\alpha)\mathcal{M}(\alpha)} \|(\mathcal{K}_1(\kappa, S) - \mathcal{K}_1(\kappa, S_n))\| \\ &\quad + \frac{2\alpha}{(2-\alpha)\mathcal{M}(\alpha)} \int_0^\kappa \|(\mathcal{K}_1(\kappa, S) - \mathcal{K}_1(\kappa, S_{n-1}))\| dy \\ &\leq \frac{2(1-\alpha)}{(2-\alpha)\mathcal{M}(\alpha)} l_1 \|S - S_{n-1}\| + \frac{2\alpha\kappa}{(2-\alpha)\mathcal{M}(\alpha)} l_1 \|S - S_{n-1}\|. \end{aligned} \tag{23}$$

Repeating the same process as above, we get

$$\|\mathcal{B}_{1n}(\kappa)\| \leq \left(\frac{2(1-\alpha)}{(2-\alpha)\mathcal{M}(\alpha)} + \frac{2\alpha\kappa}{(2-\alpha)\mathcal{M}(\alpha)}\right)^{n+1} l_1^{n+1} b. \tag{24}$$

At κ_1, we have

$$\|\mathcal{B}_{1n}(\kappa)\| \leq \left(\frac{2(1-\alpha)}{(2-\alpha)\mathcal{M}(\alpha)} + \frac{2\alpha}{(2-\alpha)\mathcal{M}(\alpha)}\kappa_1\right)^{n+1} l_1^{n+1} b. \tag{25}$$

From (24), as $n \to \infty$, gives $\|\mathcal{B}_{1n}(\kappa)\| \to 0$. Similarly,

$$\|\mathcal{B}_{2n}(\kappa)\| \to 0,\ \|\mathcal{B}_{1n}(\kappa)\| \to 0,\ \|\mathcal{B}_{3n}(\kappa)\| \to 0,\ \|\mathcal{B}_{3n}(\kappa)\| \to 0.$$

■

Next, to show the solution is unique, suppose that there exist $S_1(\kappa)$, $I_1(\kappa)$, $R_1(\kappa)$, and $V_1(\kappa)$, then

$$\begin{aligned} S(\kappa) - S_1(\kappa) = {} & \frac{2(1-\alpha)}{(2-\alpha)\mathcal{M}(\alpha)}(\mathcal{K}_1(\kappa, S) - \mathcal{K}_1(\kappa, S_1)) \\ & + \frac{2\alpha}{(2-\alpha)\mathcal{M}(\alpha)}\int_0^\kappa (\mathcal{K}_1(\kappa, S) - \mathcal{K}_1(\kappa, S_1))dy. \end{aligned} \tag{26}$$

By taking the norm of (26), and from Lemma 1, we get

$$\begin{aligned} \|S(\kappa) - S_1(\kappa)\| = {} & \frac{2(1-\alpha)}{(2-\alpha)\mathcal{M}(\alpha)}\|\mathcal{K}_1(\kappa, S) - \mathcal{K}_1(\kappa, S_1)\| \\ & + \frac{2\alpha}{(2-\alpha)\mathcal{M}(\alpha)}\int_0^\kappa \|\mathcal{K}_1(\kappa, S) - \mathcal{K}_1(\kappa, S_1))\|dy \\ \leq {} & \frac{2(1-\alpha)}{(2-\alpha)\mathcal{M}(\alpha)} l_1 \|S(\kappa) - S_1(\kappa)\| \\ & + \frac{2\alpha t}{(2-\alpha)\mathcal{M}(\alpha)} l_1 \|S(\kappa) - S_1(\kappa)\|. \end{aligned} \tag{27}$$

It simplifies to

$$\|S(\kappa) - S_1(\kappa)\|\left(1 - \frac{2(1-\alpha)}{(2-\alpha)\mathcal{M}(\alpha)} l_1 + \frac{2\alpha\kappa}{(2-\alpha)\mathcal{M}(\alpha)} l_1\right) \leq 0. \tag{28}$$

Theorem 2 *Given that the following inequality*

$$\left(1 - \frac{2(1-\alpha)}{(2-\alpha)\mathcal{M}(\alpha)} l_1 + \frac{2\alpha\kappa}{(2-\alpha)\mathcal{M}(\alpha)} l_1\right) > 0,$$

holds. Then the solution of model (10) *is unique.*

Proof Suppose that (28) holds, then

$$\|S(\kappa) - S_1(\kappa)\|\left(1 - \frac{2(1-\alpha)}{(2-\alpha)\mathcal{M}(\alpha)} l_1 + \frac{2\alpha\kappa}{(2-\alpha)\mathcal{M}(\alpha)} l_1\right) \leq 0. \tag{29}$$

Hence,

$$\|S(\kappa) - S_1(\kappa)\| = 0,$$

which leads to

$$S(\kappa) = S_1(\kappa).$$

Repeating the same techniques above can easily drive similar equality for the rest. Hence, we conclude that the solution is unique. ■

Positivity and boundedness of solution

One of the important characteristics of epidemiological models is that their solutions are both positive and bounded. In order to ensure this, we establish that all of the state variables are non-negative for any time $\kappa > 0$, which implies that a trajectory starting with a positive initial condition will stay positive for all $\kappa > 0$. Thus, system (10) gives

$$\begin{aligned} {}^{CF}D^{\alpha}S(\kappa)|_{S=0} &= \Omega + \eta V + \gamma R \geq 0, \\ {}^{CF}D^{\alpha}I(\kappa)|_{I=0} &\geq 0, \\ {}^{CF}D^{\alpha}R(\kappa)|_{R=0} &= \beta I \geq 0, \\ {}^{CF}D^{\alpha}V(\kappa)|_{V=0} &= \sigma I \geq 0. \end{aligned} \tag{30}$$

Since $N(\kappa) = S(\kappa) + I(\kappa) + R(\kappa)$ is the total human population. Thus, summing up the first three equations of (10) leads

$${}^{CF}D^{\alpha}_{0,\kappa}N(\kappa) = \Omega - \mu S - \mu I - \omega I - \sigma I - \mu R \leq \Omega - \mu S, \tag{31}$$

then one has

$$N(\kappa) \leq \left(N(0) - \frac{\Omega}{\mu}\right) E_{\alpha}(-\mu\kappa) + \frac{\Omega}{\mu}.$$

Thus, we obtain

$$\Theta = \left\{(S(\kappa), I(\kappa), R(\kappa)) \in \mathbb{R}^3_+ : 0 \leq N(\kappa) \leq \frac{\Omega}{\mu}\right\}, \tag{32}$$

which gives the biologically feasible region for the model (10). Therefore, Θ is positively invariant. Hence, the proposed model (10) is mathematically and epidemiologically well-posed.

5 Sensitivity analysis

We conducted a sensitivity analysis in this section to ascertain the contribution of each parameter to the basic reproduction number $(\mathcal{R}_0)$. This strategy determines the extent to which each parameter value contributes to the $\mathcal{R}_0$. Thus,

$$\mathcal{R}_0 = \frac{1}{\mu}\left(\lambda\Omega - (\mu + \omega + \sigma + \beta)\right),$$

is the basic reproduction number of model (10); whereas the sensitivity index of the model parameter is given by the relation

$$\Gamma_X^{\mathcal{R}_0} = \frac{\partial \mathcal{R}_0}{\partial X} \times \frac{X}{\mathcal{R}_0}.$$

The sensitivity analysis presented in Table 3 and Figure 1 examines the impact of various

Table 3. Sensitivity analysis of the parameter values

Parameters	Value	Sensitivity value
λ	0.011	0.263839
Ω	0.000096275	0.263839
μ	0.00002536	-1.062007
ω	0.0005	-0.956416
σ	15	-2.3985
β	6	-1.1992

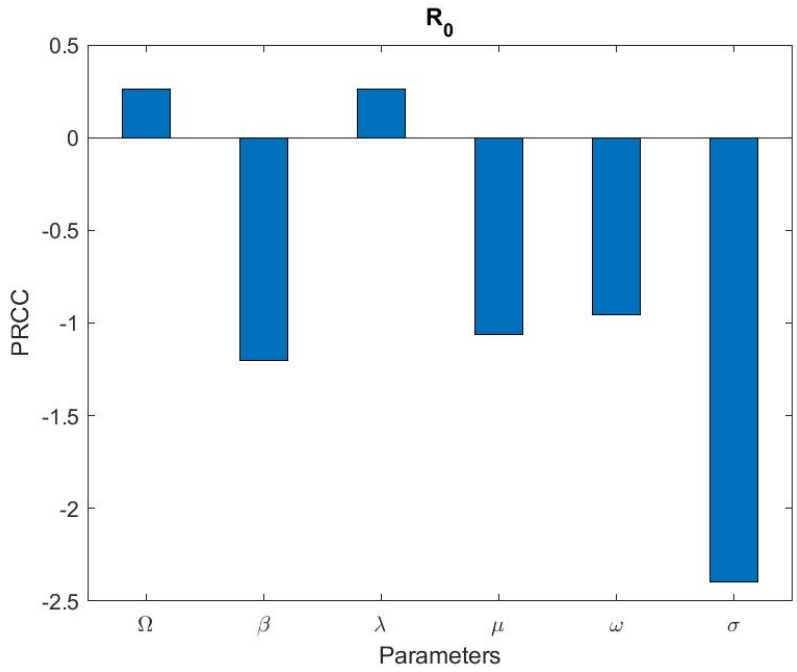

Figure 1. Sensitivity analysis of the parameter values

parameters on the $\mathcal{R}_0$. The results show that the recruitment and contact rates are the most sensitive parameters, significantly contributing to the $\mathcal{R}_0$ increase. This suggests that increasing these parameters will increase the $\mathcal{R}_0$. On the other hand, the recovery rate is less sensitive, indicating that an increase in the recovery rate will lead to a decrease in the $\mathcal{R}_0$. A response surface plot has been generated to demonstrate how the behavior of $\mathcal{R}_0$ changes when varying the values of the most sensitive parameters, as shown in Figure 2. Figure 2(a) is the plot of $\mathcal{R}_0$ versus the rate of infection σ among Infected (I) individuals and Environment (V) and recruitment rate Ω. Figure 2(b) is the plot of $\mathcal{R}_0$ versus death rate due to infection ω and recruitment rate Ω. Figure 2(c) is the plot of $\mathcal{R}_0$ versus contact rate λ and recovery rate β. Figure 2(d) is the plot of $\mathcal{R}_0$ versus contact rate λ and recruitment rate Ω.

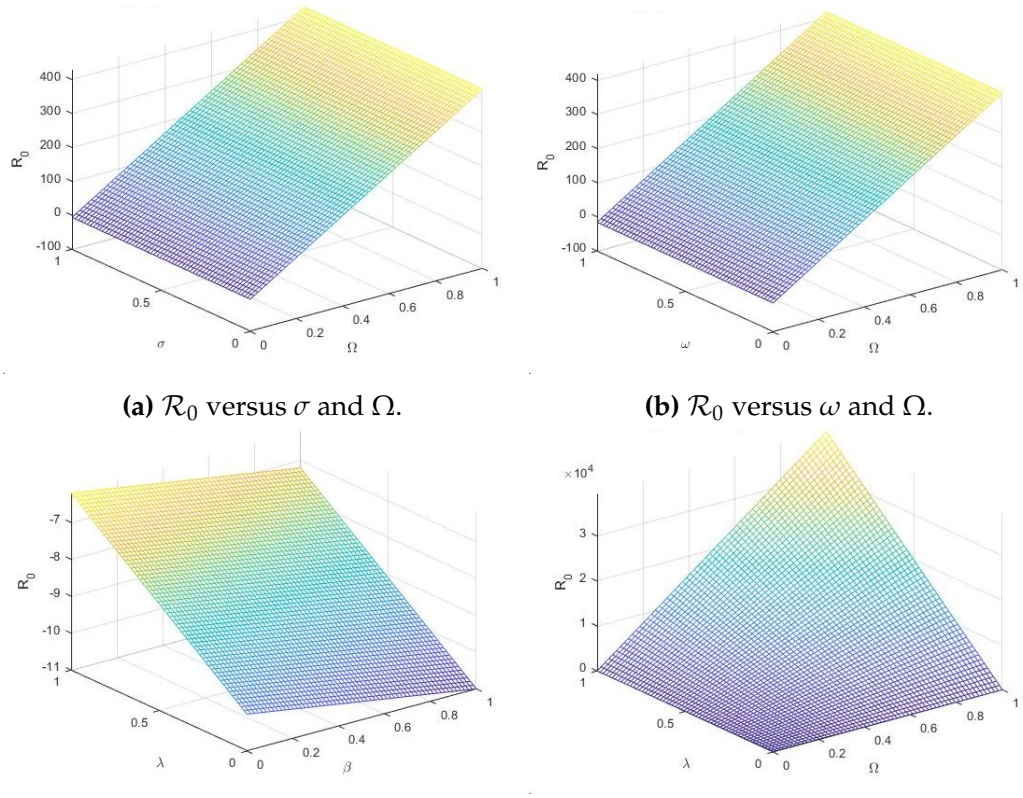

(a) $\mathcal{R}_0$ versus σ and Ω.

(b) $\mathcal{R}_0$ versus ω and Ω.

(c) $\mathcal{R}_0$ versus λ and β.

(d) $\mathcal{R}_0$ versus λ and Ω.

Figure 2. Behavior of $\mathcal{R}_0$ while varying the value of the most sensitive parameters

6 Numerical simulations and discussions

The classical and fractional-order models need numerical techniques to understand the behavior of the solution trajectories better. Here, we utilized a recent and effective numerical scheme introduced by [41] to gain insight into the solution trajectories. For a detailed analysis of this method's convergence, accuracy, and stability, please refer to [41, 42]. In Table 4, we provided the numerical values of the parameters used to find the proposed model's numerical simulations.

Interestingly, as we varied the fractional order, we observed distinct memory effects in each

Table 4. Parameters values

Parameters	Value
Ω	15
μ	0.02537
ω	0.004
β	0.0064
σ	0.0910
η	0.075
λ	0.061
γ	0.032

compartment, which were not present in the classical model, as shown in Figure 4. Figures 3 and 4 illustrate the dynamical behavior of each compartment in our study. We observed a decrease in the number of susceptible individuals as the number of recovered individuals increased over time. This trend can be attributed to the direct relationship between infectious and recovered individuals.

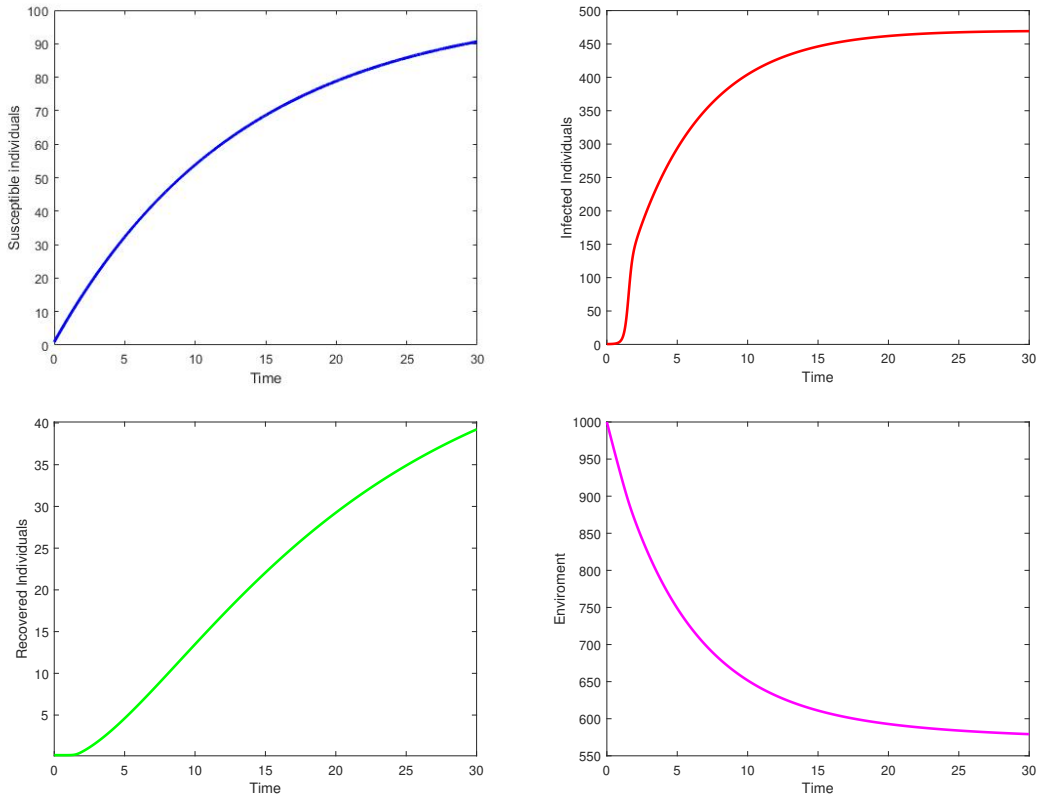

Figure 3. Classical dynamical behavior of each state variable

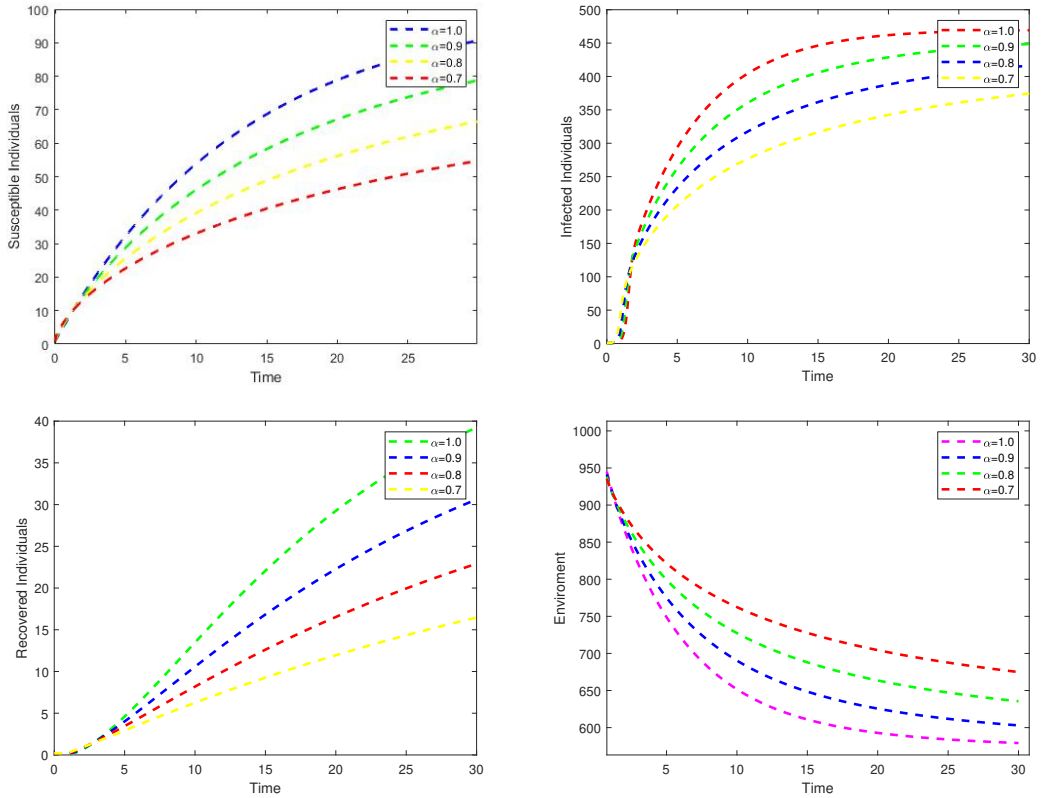

Figure 4. Caputo-Fabrizio fractional-order dynamical behavior of each state variable

Additionally, there was an increase in the concentration of bacteria, which could be linked to the contributions of infectious humans to environmental pollution. Human activities have continued to contaminate the environment, potentially contributing to the exponential increase in bacteria in the environment.

7 Conclusions

In this paper, we have successfully developed a fractional-order Cholera model to investigate the transmission dynamics of the disease using the Caputo-Fabrizio derivative and establish the existence and uniqueness of solutions via fixed point theorems. Furthermore, the sensitivity analysis of the basic reproduction number has highlighted the significant contributions of the parameters associated with the model. Specifically, the results indicate that the recruitment and contact rate are the most sensitive parameters, significantly increasing the $\mathcal{R}_0$. We conclude that these findings provide valuable insights into the factors that contribute to the transmission dynamics of cholera and can inform public health policies and strategies for controlling the transmission of the disease.
Moreover, the findings indicate that as the number of infectious individuals in the population decreases, the number of recovered individuals in the system increases. This suggests a correlation between the decline in the infected population and the rise in the number of individuals who have successfully recovered from the disease. Moreover, results suggest that the proposed model provides valuable insights into disease transmission dynamics by utilizing fractional-order derivatives, thus the policymakers can gain a deeper understanding of disease outbreaks and devise effective strategies to manage disease outbreaks.

Declarations

Ethical approval

The authors state that this research complies with ethical standards. This research does not involve either human participants or animals.

Consent for publication

Not applicable.

Conflicts of interest

The authors declare that they have no conflict of interest.

Data availability statement

Data availability is not applicable to this article as no new data were created or analysed in this study.

Funding

This research received no specific grant from any funding agency in the public, commercial, or not-for-profit sectors.

Author's contributions

I.A.: Conceptualization, Methodology, Software, Data Curation, Writing-Original draft preparation, Writing-Reviewing and Editing. A.A.: Conceptualization, Methodology, Software, Data Curation, Writing-Original draft preparation, Visualization, Investigation, Writing-Reviewing and Editing. F.J.:Conceptualization, Methodology, Software, Writing-Reviewing and Editing.

Conceptualization, Methodology, Software, Data Curation, Writing-Original draft preparation, Visualization, Investigation. P.K.: Data Curation, Writing-Original draft preparation, Visualization, Investigation, Writing-Reviewing and Editing. K.N.: Data Curation, Writing-Original draft preparation, Visualization, Investigation, Writing-Reviewing and Editing. All authors discussed the results and contributed to the final manuscript.

Acknowledgements

The authors are thankful for the feedback provided by the anonymous reviewers and editor, which has enhanced the accuracy and readability of the paper. The first author acknowledged the support by Tertiary Education Trust Fund (TETFund) and Sule Lamido University for financial support under Post-Doctoral Fellowship.

References

[1] Acosta, C.J., Galindo, C.M., Kimario, J., Senkoro, K., Urassa, H., Casals, C. et al. Cholera outbreak in southern Tanzania: risk factors and patterns of transmission. *Emerging Infectious Diseases*, 7, 583-587, (2001). [CrossRef]

[2] Luquero, F.J., Rondy, M., Boncy, J., Munger, A., Mekaoui, H., Rymshaw, E. et al. Mortality rates during cholera epidemic, Haiti, 2010–2011. *Emerging Infectious Diseases*, 22(3), 410-416, (2016). [CrossRef]

[3] Mgonja, D.S., Massawe, E.S. and Makinde, O.D. Computational modelling of Cholera Bacteriophage with treatment. *Open Journal of Epidemiology*, 5(3), 172-186, (2015). [CrossRef]

[4] Moore, M., Gould, P. and Keary, B.S. Global urbanization and impact on health. *International Journal of Hygiene and Environmental Health*, 206(4-5), 269-278, (2003). [CrossRef]

[5] Biswas, D. and Pal, S. Role of awareness to control transmission of HIV/AIDS epidemic with treatment and sensitivity analysis. *Journal of Statistics and Management Systems*, 25(3), 617-644, (2022). [CrossRef]

[6] Abimbade, S.F., Olaniyi, S., Ajala, O.A. and Ibrahim, M.O. Optimal control analysis of a tuberculosis model with exogenous re-infection and incomplete treatment. *Optimal Control Applications and Methods*, 41(6), 2349-2368, (2020). [CrossRef]

[7] Mukandavire, Z., Garira, W. and Tchuenche, J.M. Modelling effects of public health educational campaigns on HIV/AIDS transmission dynamics. *Applied Mathematical Modelling*, 33(4), 2084-2095, (2009). [CrossRef]

[8] Ahmed, I., Yusuf, A., Ibrahim, A., Kumam, P., and Ibrahim, M. J. A mathematical model of the ongoing coronavirus disease (COVID-19) pandemic: a case study in Turkey. *Science and Technology Asia*, 27(4), 248-258, (2022). [CrossRef]

[9] Peter, O.J., Qureshi, S., Yusuf, A., Al-Shomrani, M. and Idowu, A.A. A new mathematical model of COVID-19 using real data from Pakistan. *Results in Physics*, 24, 104098, (2021). [CrossRef]

[10] Layton, A.T. and Sadria, M. Understanding the dynamics of SARS-CoV-2 variants of concern in Ontario, Canada: a modeling study. *Scientific Reports*, 12, 2114, (2022). [CrossRef]

[11] Duran, S., Durur, H., Yavuz, M. and Yokus, A. Discussion of numerical and analytical techniques for the emerging fractional order murnaghan model in materials science. *Optical and Quantum Electronics*, 55, 571, (2023). [CrossRef]

[12] Sun, G.Q., Xie, J.H., Huang, S.H., Jin, Z., Li, M.T. and Liu, L. Transmission dynamics of cholera: mathematical modeling and control strategies. *Communications in Nonlinear Science*

and Numerical Simulation, 45, 235-244, (2017). [CrossRef]

[13] Senderovich, Y., Izhaki, I. and Halpern, M. Fish as reservoirs and vectors of Vibrio cholerae. *PloS one*, 5(1), e8607, (2010). [CrossRef]

[14] Islam, M.S., Zaman, M.H., Islam, M.S., Ahmed, N. and Clemens, J.D. Environmental reservoirs of Vibrio cholerae. *Vaccine*, 38, A52-A62, (2020). [CrossRef]

[15] Chac, D., Dunmire, C.N., Singh, J. and Weil, A.A. Update on environmental and host factors impacting the risk of Vibrio cholerae infection. *ACS Infectious Diseases*, 7(5), 1010-1019, (2021). [CrossRef]

[16] Tilahun, G.T., Woldegerima, W.A. and Wondifraw, A. Stochastic and deterministic mathematical model of cholera disease dynamics with direct transmission. *Advances in Difference Equations*, 2020, 670, (2020). [CrossRef]

[17] Adewole, M.O. and Faniran, T.S. Analysis of Cholera model with treatment noncompliance. *International Journal of Nonlinear Analysis and Applications*, 13(1), 29-43, (2022). [CrossRef]

[18] Diethelm, K. and Ford, N.J. Analysis of fractional differential equations. *Journal of Mathematical Analysis and Applications*, 265(2), 229-248, (2002). [CrossRef]

[19] Kilbas, A.A., Srivastava, H.M. and Trujillo, J.J. *Theory and Applications of Fractional Differential Equations* (Vol. 204). Elsevier: Netherlands, (2006).

[20] Uçar, S., Evirgen, F., Özdemir, N. and Hammouch, Z. Mathematical analysis and simulation of a giving up smoking model within the scope of non-singular derivative. In Proceedings, *Institute of Mathematics and Mechanics, National Academy of Sciences of Azerbaijan* (Vol. 48) pp. 84–99, Baku, Azerbaijan, (2022). [CrossRef]

[21] Uçar, S. Existence and uniqueness results for a smoking model with determination and education in the frame of non-singular derivatives. *Discrete and Continuous Dynamical Systems Series S*, 14(7), 2571-2589, (2021). [CrossRef]

[22] Uçar, E. and Özdemir, N. A fractional model of cancer-immune system with Caputo and Caputo–Fabrizio derivatives. *The European Physical Journal Plus*, 136, 1-17, (2021). [CrossRef]

[23] Yokus, A., Durur, H., Kaya, D., Ahmad, H. and Nofal, T.A. Numerical comparison of Caputo and Conformable derivatives of time fractional Burgers-Fisher equation. *Results in Physics*, 25, 104247, (2021). [CrossRef]

[24] Ahmad, S., Dong, Q.I.U. and Rahman, M.U. Dynamics of a fractional-order COVID-19 model under the nonsingular kernel of Caputo-Fabrizio operator. *Mathematical Modelling and Numerical Simulation with Applications*, 2(4), 228-243, (2022). [CrossRef]

[25] Atede, A.O., Omame, A. and Inyama, S.C. A fractional order vaccination model for COVID-19 incorporating environmental transmission: a case study using Nigerian data. *Bulletin of Biomathematics*, 1(1), 78-110, (2023). [CrossRef]

[26] Ullah, S., Khan, M.A., Farooq, M., Hammouch, Z. and Baleanu, D. A fractional model for the dynamics of tuberculosis infection using Caputo-Fabrizio derivative. *Discrete and Continous Dynamical System Series S*, 13(3), (2020). [CrossRef]

[27] Özköse, F., Habbireeh, R. and Şenel, M.T. A novel fractional order model of SARS-CoV-2 and Cholera disease with real data. *Journal of Computational and Applied Mathematics*, 423, 114969, (2023). [CrossRef]

[28] Ahmed, I., Goufo, E.F.D., Yusuf, A., Kumam, P., Chaipanya, P. and Nonlaopon, K. An epidemic prediction from analysis of a combined HIV-COVID-19 co-infection model via

ABC-fractional operator. *Alexandria Engineering Journal*, 60(3), 2979-2995, (2021). [CrossRef]

[29] Ahmed, I., Yusuf, A., Sani, M.A., Jarad, F., Kumam, W. and Thounthong, P. Analysis of a Caputo HIV and malaria co-infection epidemic model. *Thai Journal of Mathematics*, 19(3), 897-912, (2021).

[30] Din, A., Li, Y., Yusuf, A., Liu, J. and Aly, A.A. Impact of information intervention on stochastic hepatitis B model and its variable-order fractional network. *The European Physical Journal Special Topics*, 231, 1859-1873, (2022). [CrossRef]

[31] Addai, E., Zhang, L., Preko, A.K. and Asamoah, J.K.K. Fractional order epidemiological model of SARS-CoV-2 dynamism involving Alzheimer's disease. *Healthcare Analytics*, 2, 100114, (2022). [CrossRef]

[32] Hanif, A., Butt, A.I.K., Ahmad, S., Din, R.U. and Inc, M. A new fuzzy fractional order model of transmission of Covid-19 with quarantine class. *The European Physical Journal Plus*, 136, 1179, (2021). [CrossRef]

[33] Uçar, S., Özdemir, N., Koca, İ. and Altun, E. Novel analysis of the fractional glucose–insulin regulatory system with non-singular kernel derivative. *The European Physical Journal Plus*, 135, 414, (2020). [CrossRef]

[34] Duran, S., Yokuş, A. and Durur, H. Surface wave behavior and refraction simulation on the ocean for the fractional Ostrovsky–Benjamin–Bona–Mahony equation. *Modern Physics Letters B*, 35(31), 2150477, (2021). [CrossRef]

[35] Durur, H., Yokuş, A. and Yavuz, M. Behavior analysis and asymptotic stability of the traveling wave solution of the Kaup-Kupershmidt equation for conformable derivative. In *Fractional Calculus: New Applications in Understanding Nonlinear Phenomena* (Vol. 3) pp. 162-185, (2022). [CrossRef]

[36] Joshi, H., Yavuz, M. and Stamova, I. Analysis of the disturbance effect in intracellular calcium dynamic on fibroblast cells with an exponential kernel law. *Bulletin of Biomathematics*, 1(1), 24-39, (2023). [CrossRef]

[37] Rashid, S., Jarad, F., Alsubaie, H., Aly, A.A. and Alotaibi, A. A novel numerical dynamics of fractional derivatives involving singular and nonsingular kernels: designing a stochastic cholera epidemic model. *AIMS Mathematics*, 8(2), 3484-3522, (2023). [CrossRef]

[38] Baleanu, D., Jajarmi, A., Mohammadi, H. and Rezapour, S. A new study on the mathematical modelling of human liver with Caputo–Fabrizio fractional derivative. *Chaos, Solitons and Fractals*, 134, 109705, (2020). [CrossRef]

[39] Losada, J. and Nieto, J.J. Properties of a new fractional derivative without singular kernel. *Progress in Fractional Differentiation and Applications*, 1(2), 87-92, (2015).

[40] Eustace, K.A., Osman, S. and Wainaina, M. Mathematical modelling and analysis of the dynamics of cholera. *Global Journal of Pure and Applied Mathematics*, 14(9), 1259-1275, (2018).

[41] Atangana, A. and Owolabi, K.M. New numerical approach for fractional differential equations. *Mathematical Modelling of Natural Phenomena*, 13(1), 3, (2018). [CrossRef]

[42] Evirgen, F., Uçar, E., Uçar, S. and Özdemir, N. Modelling influenza a disease dynamics under Caputo-Fabrizio fractional derivative with distinct contact rates. *Mathematical Modelling and Numerical Simulation with Applications*, 3(1), 58-72, (2023). [CrossRef]

Mathematical Modelling and Numerical Simulation with Applications (MMNSA)
(https://dergipark.org.tr/en/pub/mmnsa)

How to cite this article: Ahmed, I., Akgül, A., Jarad, F., Kumam, P. & Nonlaopon, K. (2023). A Caputo-Fabrizio fractional-order cholera model and its sensitivity analysis. *Mathematical Modelling and Numerical Simulation with Applications,* 3(2), 170-187. https://doi.org/10.53391/mmnsa.1293162